

REMOTE SENSING METHODS TO DETECT AND IDENTIFY CLAY-MADE HOUSES

H. Khawary ^{1*}, P. Zeaieanfiroozabadi ¹, J. Sadidi ¹

¹Dept. of Remote Sensing and GIS, Kharazmi University, Tehran, Iran - (Std_Hkhawary, zeaiean, jsadidi)@khu.ac.ir

Commission IV, WG IV/3

KEY WORDS: Remote sensing, Data fusion, Classification, Radar, Thermal Data, Yazd.

ABSTRACT:

One of the most important issues in urban management is the existence of clay-made houses in or around cities. By the hypothesis that these phenomena are spectrally and spatially behaviour differently from other land uses and land covers. This study attempts to detect and identify clay-made houses through different image processing methods. In this regard, Sentinel 1, 2, and Landsat 8 OLI thermal images of Yazd city have been analysed. After pre-processing, a number of image processing techniques, including optical and radar image composite generation, band ratio, image fusion, image filtering, and image classification (i.e. MLC and ANN), have been used. The result shows that RGB from a combination of Red=radar band C, Green=sentinel band 8, and Blue=sentinel band 4 are the best for visual interpretation of clay-made houses. Also, the most suitable band ratio is the ratio corresponding to radar C and NIR, the Red and Green bands, and the best fusion is derived with Sentinel 1 (band C) and Sentinel 2 (bands 4 and 8) images through the HSV algorithm, kappa coefficients of the agreement for MLC and ANN classifiers are 0.89 and 0.29 respectively. It is concluded that remote sensing image analysis can effectively be used to detect and identify clay-made houses.

1. INTRODUCTION

It has been demonstrated that remote sensing techniques can detect and identify different materials on the earth's surface. It can detect different materials through image processing techniques such as enhancement analysis, and active and passive image fusion. However, there has been little research work on identifying clay-made houses with remote sensing. In developing countries like Iran, most clay-made houses are the heritage of the past, and some of them have been built illegally. Collecting and gathering information about their spatial distribution, area, etc., is essential for crisis management, health, education, tourism, and other services.

Here, to detect and identify clay-made houses, different remote sensing sources such as Sentinel 1, Sentinel 2, and Landsat 8-OLI have been used. After implementing careful pre-processing techniques, several different image processing analyses, including image enhancement, image fusion, and classification algorithms, have been carried out.

2. MATERIALS AND METHODS

2.1 Research Area

In the center of Iran, the province of Yazd occupies an area of 131,575 square kilometers. Yazd city, which is Yazd province's capital, has an altitude of 1230 meters over the mean sea level. Moreover, it is located at 31° 90' N and 54° 37' E coordinates. As a result of Yazd's hot and dry climate, temperatures fluctuate greatly between winter and summer as well as from day to night (Mostafaeipour et al., 2014), Figure 1.

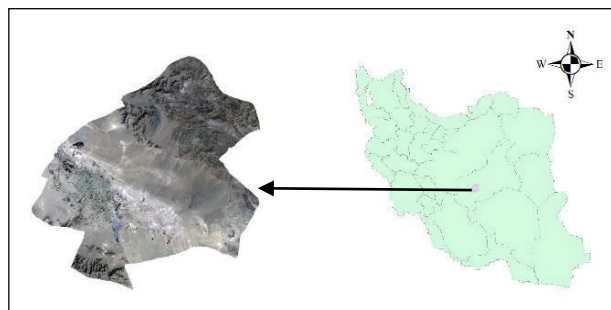


Figure 1. Area under study in Yazd province, Iran.

2.2 Data Acquisition

Sentinel-1, dated 05 May 2022, and Sentinel-2 acquired on 11 May 2022 were obtained for this study from European Space Agency (ESA). The image processing application ENVI 5.3 was used for both images. Table 1 presents the characteristics of both data sets.

	Sentinel-1a	Sentinel-2 (Level-1C)
Acquisition date	2022/05/05	2022/05/11
Ground resolution	5×20	10 m, 20 m, 60 m
Coverage	400 km	100 km ²
Band Number	C	2, 3, 4, 5, 6, 7, 8

Table 1. Data characteristics.

* Corresponding author

3. METHODOLOGY

3.1 Data Analysis and Image Processing

3.1.1 Clay-made houses Detection Technique

3.1.1.1 Band Combination Technique: Band composite generation was employed for the image following pre-processing. This technique allows for the selection of specific bands from the satellite image for the purpose of creating a colour image that facilitates the identification of features. (Younggu and Conrade, 2007). Different combinations of image bands were applied (Figure 2). Results indicate that combining band C as a red channel from radar data, band 8 as a green channel, and band 4 as a blue channel from Sentinel data would provide a better appearance of three main features.

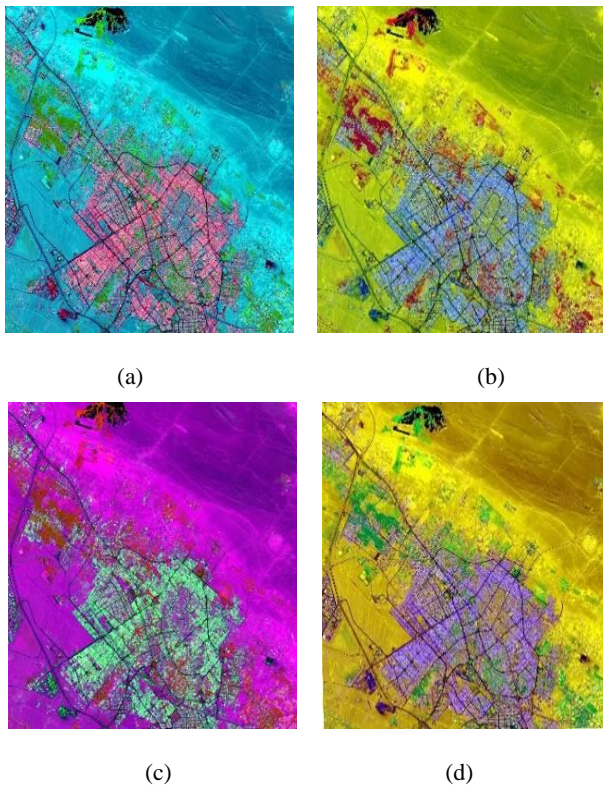


Figure 2. Band Combination technique for Sentinel 1, 2 images: (a) Band C, 8, 4 (b) Band 8, 4, C (c) Band 8, C, 4 (d) Band 4, 8, C.

3.1.1.2 Band Ratio Techniques: Compared to enhancement and band combination techniques, the band ratio method provided a more detailed image of the houses. Houses' spectral characteristics will be enhanced by the combinations of band ratios used (Asmat and Zamzami, 2011). Ratios between Red (Band4), Green (Band3), Near-infrared (NIR) (Band8), and C (Radar) were applied to the Sentinel1 and 2 images. According to the results, the best band ratio is the ratio between the C and NIR bands, the Red, and Green bands, which will then be used for further analysis. According to Figure 3, the three classes of house, water, and land can be separated accurately using this combination.

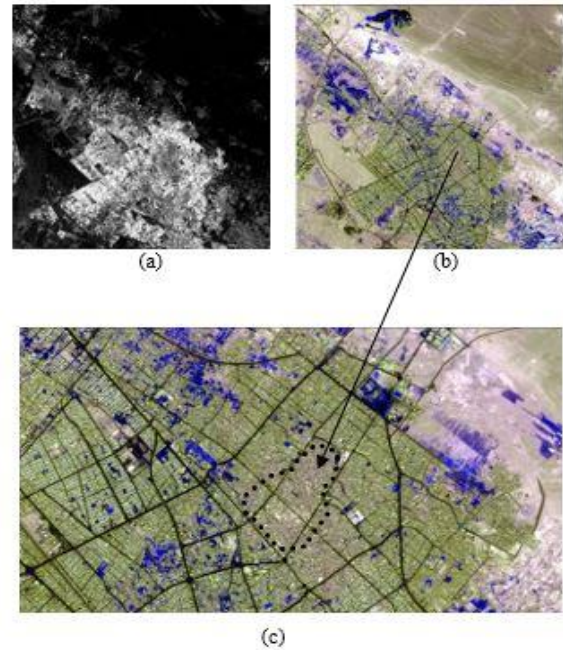


Figure 3. Band ratio of C/NIR band Red/Green (a, b, and c).

3.1.1.3 Enhancement Techniques: To optimize the image for analysis and visual interpretation, different enhancement types were applied to it, including linear, root, equal, adaptive, and infrequency functions. By stretching the maximum and minimum of the image digital values over the total dynamic range, linear enhancement optimizes the images' overall contrast (Asmat and Zamzami, 2011). As shown in Figure 4, by modifying certain components, different subbands can be created, and the contrast can be enhanced (Celik, 2012). To modify the brightness of an image, a singular value equalization approach is proposed in (Demirel et al. 2008). Moreover, in (Demirel et al., 2010), this technique is further developed by adding discrete wavelet transforms. An alternative method is presented in (Lee et al., 2013), in which discrete wavelet transforms are combined with adaptive intensity transformations in order to enhance contrast in remote sensing images. This method is not suitable for practical use, as it requires appropriate parameter settings. As a method for enhancing optical remote sensing images, a subband-decomposed multiscale retinex technique based on a hybrid intensity transfer function is presented in (Jang et al., 2011). Using multiple remote sensing images, a method of general illumination normalization is proposed by Zhang et al., (2014). In this technique, the contrast is initially enhanced in the gradient domain, and after that, the singular value is equalized in order to alter the brightness.

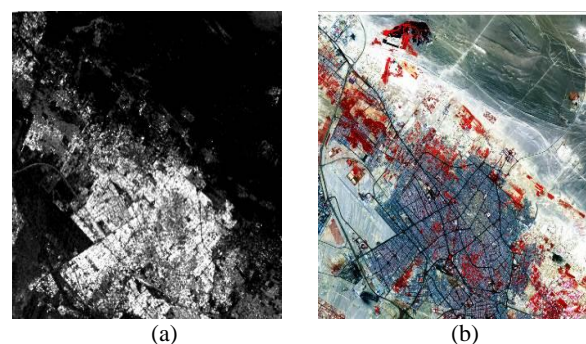
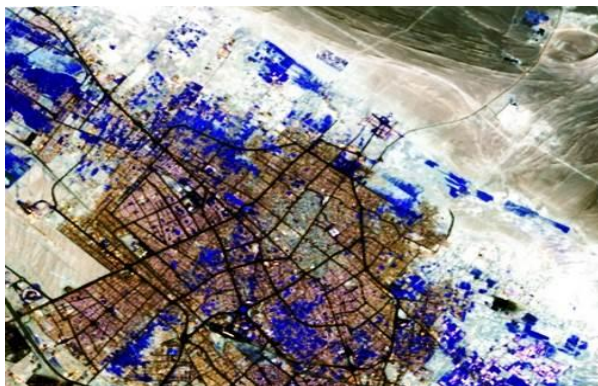


Figure 4. Percentage linear enhancement of 5% in the image: (a) Sentinel-1 (b) Sentinel-2.

3.1.1.3 Filtering Techniques: The image filtering techniques are effective for identifying the form of the clay-made houses found within the Sentinel images. House edges should be separated by the best filter types (Asmat and Zamzami, 2011). Here, different spatial domain edge detection filters have been tested. Sentinel imagery was first filtered with a 3 X 3 local sigma filter to delineate the house's edge. Following this, to determine the inner diameter of the high-intensity house area, a 7 X 7 edge-enhanced Lee filter is applied. Lastly, a threshold image method was then used to identify the particular house centroid. Results indicate that houses are clearly separated from one another and that delineating houses can be done within 10 meters of each other. Figure 5 shows how the local sigma filter provided superior results and was able to separate the houses' edges accurately.



(a)



(b)



(c)

Figure 5. (a) Local sigma filter, (b) Enhanced lee filter, (c) Kuan filter.

3.1.2 Clay-made Houses Extraction

3.1.2.1 Application of Thermal Images: Typically, land surface temperature (LST) is measured from a remote sensing thermal band and provides a specific response to landscape dynamics, including Land Cover categorization and Land Cover modification (El-Zeiny and Effat, 2017; Sinha et al., 2014). Using thermal infrared imagery, quantitative details about Ts can be obtained within different Land Cover groups (Sinha et al., 2015; Sinha et al., 2014). Biological and physicochemical structures on Earth interact with the LST in complex ways (Becker and Li, 1990; Li et al., 2004). Therefore, LST is the primary measure in determining the biological and physicochemical properties of land surface structures, energy flows, and interplanetary interactions between the atmosphere and the planet (Sobrino et al., 2003). As a result, it can provide vital information about the climatic and physical characteristics of the surface, which are vital across a wide range of environmental procedures (Weng, 2011; Zhang et al., 2015). The RS data is, therefore, an important variable in meteorological and climatological studies. Climate change, however, is associated with increased land cover and human activity. There are detailed dynamics and an explanation of how the LST works in (Dash et al., 2001; Dash et al., 2002). Due to its high resolution, continuous, revisited coverage, and capacity to measure the surface requirements of the Earth, satellite imagery is the best method for obtaining LST parameters, both regionally and internationally (Owen et al., 1998).

The principles behind thermal remote sensing differ from those behind microwave and optical remote sensing. Other remote sensing data are complementary to thermal data in practice. As a result, thermal remote sensing offers a variety of applications, despite not being fully explored (Prakash, 2000). The temperature of clay-made houses is different from the temperature of non-clay houses, and this helps us identify clay-made houses, Figure 6. Also, the thermal reflectance diagram using Landsat 8-Oli, band 10, is shown in Figure 7.

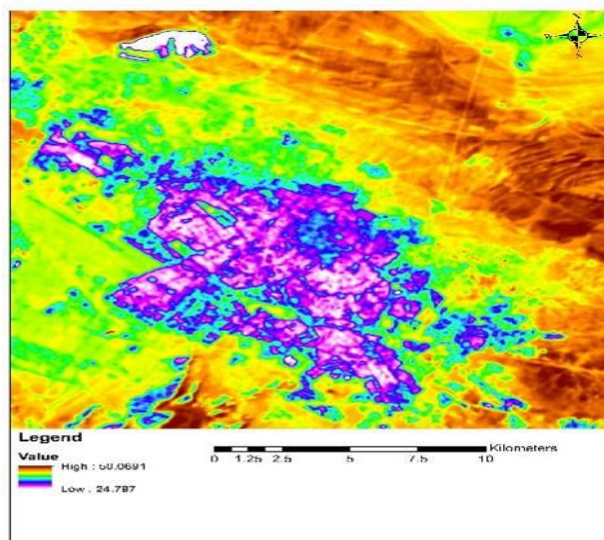
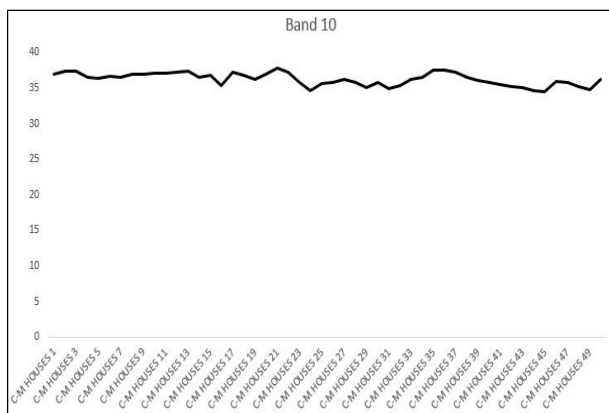
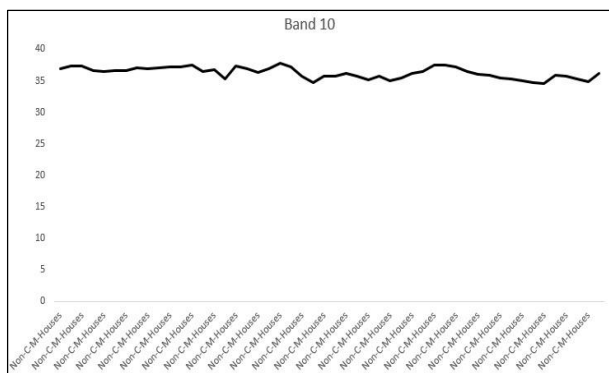


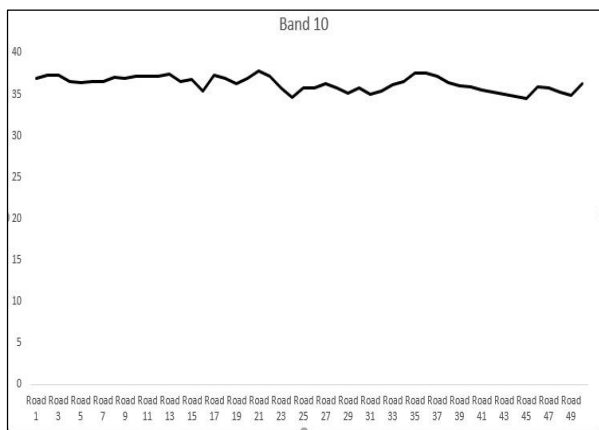
Figure 6. Thermal image of Yazd city clay- made houses have less temperature than surrounding areas (purple colour).



(a)



(b)



(c)

Figure 7. Thermal reflectance diagram of Landsat8-Oli, Band 10: (a) Clay Made-House, (b) Non Clay-made House, (c) Road.

3.1.2.2 Data Fusion: This colour model is based on human visualization, perception, and knowledge of the concept of colour and is defined based on the space of cylindrical coordinates. The importance of cylindrical colour systems in image processing is due to the separation of light intensity from the colour, which allows the combination of different data with each other (Sharifikia et al., 2020). Here, the Sentinel 1 (band C) and Sentinel 2 (bands 4 and 8) images are integrated using the data fusion HSV algorithm, Figure 8.

The following is the straightforward, most popular, and probably most intuitive approach to employ (Subramanian et al., 2015):

1. From the multispectral imagery, select three spectral bands.

2. Sync the low-resolution colour image with the high-resolution panchromatic image (i.e., magnifying the colour image as it is in the panchromatic image in terms of pixel size).

3. Convert the magnified colour image from RGB to HSV (which stands for Hue Saturation Value).

4. Put the high-resolution panchromatic image in place of the value image.

5. Reverse the image to RGB using the HSV matrix expression method as follows:

First, transform RGB to HSV by applying:

$$\begin{bmatrix} V \\ V_1 \\ V_2 \end{bmatrix} = \begin{bmatrix} 0.577 & 0.577 & 0.577 \\ -0.408 & -0.408 & 0.816 \\ -0.707 & 0.707 & 1.703 \end{bmatrix} \begin{bmatrix} R \\ G \\ B \end{bmatrix} \quad (1)$$

$$H = \tanh^{-1} \left(\frac{v_1}{v_2} \right) \quad (2)$$

$$S = \sqrt{V_2^2 + V_1^2} \quad (3)$$

For each pixel in a color image, the gray value in its Pan image is used. In other words, for the previous equations (1, 2, 3), consider $V=I$.

Second, transform HSV to RGB by applying:

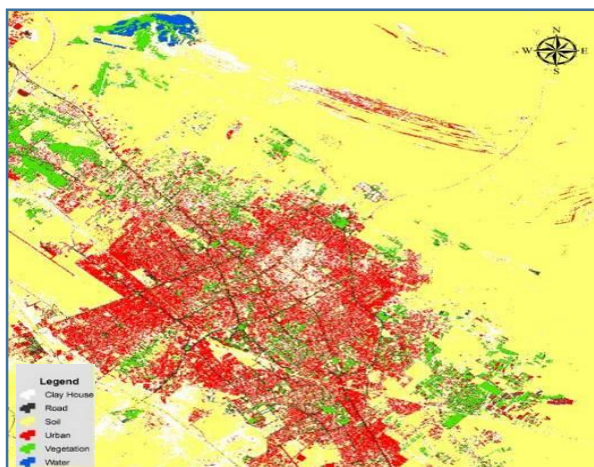
$$\begin{bmatrix} R \\ G \\ B \end{bmatrix} = \begin{bmatrix} 0.577 & -0.408 & -0.707 \\ 0.577 & -0.408 & 0.816 \\ 0.577 & 0.816 & 0 \end{bmatrix} \begin{bmatrix} V \\ V_1 \\ V_2 \end{bmatrix} \quad (4)$$



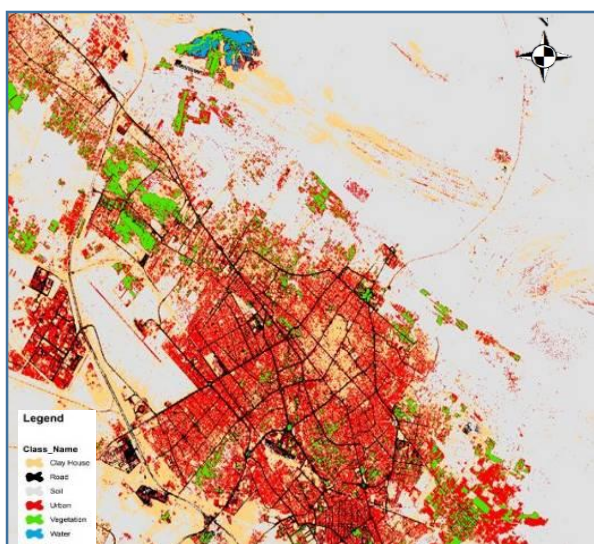
Figure 8. Data fusion, HSV algorithm.

3.1.2.3 Image Classification analysis: One of the most commonly employed remote sensing applications is the classification and processing of satellite images to map land use and cover. Satellite images can be classified using a variety of algorithms. Classification techniques can be categorized into object-based and pixel-based techniques. One of the most widely used and reliable methods for classifying remote sensing data is the Maximum Likelihood method. A pixel is assigned to the class with the highest probability. For supervised image classification, neural networks are most widely utilized (Atkinson and Tatnall, 1997; Wilkinson, 1997). The Artificial Neural Network (ANN) classification is based on mathematical activation functions and tries to find weights to reach the best final outputs. Mixed pixel and image speckle problems can be reduced by ANN (Mustapha et al. 2010). To identify the spatial distribution of clay-made houses, a supervised NN classifier was utilized (Figure 9). A majority voting strategy is used for classifying each network, in which the class with the maximum number of votes is taken

from all networks and allocated to the sample. The Dempster-Shafer theory of evidence can also be combined and used in more complex versions of this strategy (Rogova 1994). As a result of the experiments conducted in this study, the Maximum Likelihood method with a Kappa Coefficient of 0.89 is more reliable than the Neural Networks with a Kappa coefficient of 0.29 in Table 2.



(a)



(b)

Figure 9. (a) Neural network Classification output, (b) Maximum likelihood Classification output.

Algorithm Classification	Kappa Coefficient
Maximum likelihood	0.89
Neural network	0.29

Table 2. Kappa coefficient for maximum likelihood classification algorithms and neural network.

4. CONCLUSIONS

Based on this study, Remote sensing data and methods showed their ability to detect and identify clay-made houses. Several remote sensing techniques, including image enhancements, band

ratio, filtering, fusion, and classification, were implemented. The result shows that RGB from a combination of Red=sentinel band C, Green=sentinel band 8, and Blue=sentinel band 4 are the best for visual interpretation of clay-made houses. Also, the optimal band ratio is the ratio within C and NIR, the Red and Green bands, the best fusion is derived with Sentinel 1 (band C), and Sentinel 2 (bands 4 and 8) images through the HSV algorithm, kappa coefficients of the agreement for MLC and ANN classifiers are 0.89 and 0.29 respectively. It is concluded that remote sensing image analysis can effectively be used to detect and identify clay-made houses.

5. REFERENCES

- Asmat, A., Zamzami, S., 2011: Automated house detection and delineation using optical remote sensing technology for informal human settlement. *Bandung*, 15–17.
- Atkinson, P. M., Tatnall, A. R. L., 1997: Neural networks in remote sensing. *International Journal Remote Sensing*, 18, 711–725.
- Becker, F., Li, Z-L., 1990: Temperature-independent spectral indices in thermal infrared bands. *Remote sensing of environment*, 32(1), 17–33.
- Celik, T., 2012: Two-dimensional histogram equalization and contrast enhancement. *Pattern Recog.*, 45(10), 3810–3824.
- Dash, P., Göttsche, F. M., Olesen, F. S., Fischer, H., 2001: Retrieval of land surface temperature and emissivity from satellite data: physics, theoretical limitations and current methods. *Journal of the Indian Society of Remote Sensing*, 29(1-2), 23.
- Dash, P., Göttsche, F. M., Olesen, F. S., Fischer, H., 2002: Land surface temperature and emissivity estimation from passive sensor data: Theory and practice-current trends. *International Journal of remote sensing*, 23(13), 2563–94.
- Demirel, H., Anbarjafari, G., Jahromi, M. N. S., 2008: Image equalization based on singular value decomposition. *In Proc. IEEE 23rd ISICIS*, 1–5.
- Demirel, H., Ozcinar, C., Anbarjafari, G., 2010: Satellite image contrast enhancement using discrete wavelet transform and singular value decomposition. *IEEE Geosci. Remote Sens. Lett.*, 7(2), 333–337.
- El-Zeiny, A. M., Effat H. A., 2017: Environmental monitoring of spatiotemporal change in land use/land cover and its impact on land surface temperature in El-Fayoum governorate, Egypt. *Remote Sensing Applications: Society and Environment*, 8, 266–77.
- Jang, J. H., Kim, S. D., Ra, J. B., 2011: Enhancement of optical remote sensing images by subband-decomposed multiscale retinex with hybrid intensity transfer function. *IEEE Geosci. Remote Sens. Lett.*, 8(5), 983–987.
- Lee, E., Kim, S., Kang, W., Seo, D., Paik, J., 2013: Contrast enhancement using dominant brightness level analysis and adaptive intensity transformation for remote sensing images. *IEEE Geosci. Remote Sens. Lett.*, 10(1), 62–66.

- Li, F., Jackson, T. J., Kustas, W. P., Schmugge, T. J., French, A. N., Cosh, M. H., et al., 2004: Deriving land surface temperature from Landsat 5 and 7 during SMEX02/SMACEX. *Remote sensing of environment*, 92(4), 521–34.
- Mostafaiepour, A., Bardel, B., Mohammadi, K., Sedaghat, A., Dinpashoh, Y., 2014: Economic evaluation for cooling and ventilation of medicine storage warehouses utilizing wind catchers, renewable and sustainable energy reviews. *ELSEVIER*, doi.org/10.1016/j.rser.2014.05.087.
- Mustapha, M.R., Lim, S., Mat, Jafri, M.Z., 2010: Comparison of neural network and maximum likelihood approaches in image classification. *Journal of Applied Sciences* 10, 2847–2854.
- Owen, T., Carlson, T., Gillies, R., 1998: Remotely sensed surface parameters governing urban climate change. *International Journal Remote Sens*, 19, 1663–81.
- Parkash, A., 2000: Thermal Remote Sensing: concepts, issues and applications, ITC, Geological Survey Division, International Archives of Photogrammetry and Remote Sensing, Amsterdam.
- Rogova, G., 1994, Combining the results of several neural network classi@ers. *Neural Networks*, 7, 777–781.
- Sharifikia, M., Karami, J., Falahati, E., 2020: Capability assessment for RADAR and OPTIC data fusion and integrating methods to identify alteration areas. *Scientific Quarterly Journal of Geosciences*, 30(3).
- Sinha, S., Pandey, P. C., Sharma L. K., Nathawat M. S., Kumar, P., Kanga, S., 2014: Remote estimation of land surface temperature for different LULC features of a moist deciduous tropical forest region. *Remote Sensing Applications in Environmental Research: Springer*, 57–68.
- Sinha, S., Sharma, L. K., Nathawat, M. S., 2015: Improved Land-use/Land-cover classification of semi-arid deciduous forest landscape using thermal remote sensing. *The Egyptian Journal of Remote Sensing and Space Science*, 18(2), 217–33.
- Sobrino, J., El Kharraz, J., Li, Z. L., 2003: Surface temperature and water vapour retrieval from MODIS data. *International Journal of Remote Sensing*, 24(24), 5161–82.
- Subramanian, P., Alamelu, N. R., Aramudhan, M., 2015: Fusion Of Multispectral And Panchromatic Images And Its Quality Assessment. *ARPJ Journal of Engineering and Applied Sciences*, 10(9), 1819–6608.
- Wang, W., Huang, D., Wang, X. G., Liu, Y. R., Zhou, F., 2011: Estimation of soil moisture using trapezoidal relationship between remotely sensed land surface temperature and vegetation index. *Hydrology and Earth System Sciences*, 15(5), 1699–712.
- Weng, Q., 2011: Advances in environmental remote sensing: sensors, algorithms, and applications. *CRC Press*.
- Younggu, H., Conrade, H., 2007: Landuse classification in Zambia using Quickbird and Landsat Imagery. *American Society of Agricultural and Biological Engineers*.
- Zhang, G., Chen, Q., Sun, Q., 2014: Illumination normalization among multiple remote-sensing images. *IEEE Geosci. Remote Sens. Lett.*, 11(9), 1470–1474.
- Zhang, H., Weng, Q., Lin, H., Zhang, Y., 2015: Remote sensing of impervious surfaces in tropical and subtropical areas. *CRC Press*.